AIP Advances

The Schottky barrier modulation at PtSi/Si interface by strain and structural deformation

Pooja Srivastava, Mincheol Shin, Kwang-Ryeol Lee, Hiroshi Mizuseki, and Seungchul Kim

Citation: AIP Advances **5**, 087109 (2015); doi: 10.1063/1.4928323
View online: http://dx.doi.org/10.1063/1.4928323
View Table of Contents: http://scitation.aip.org/content/aip/journal/adva/5/8?ver=pdfcov
Published by the AIP Publishing

The Schottky barrier modulation at PtSi/Si interface by strain and structural deformation

Pooja Srivastava,[1] Mincheol Shin,[2] Kwang-Ryeol Lee,[1] Hiroshi Mizuseki,[1] and Seungchul Kim[1]
[1]*Center for Computational Science, Korea Institute of Science and Technology (KIST), Seoul, 136-791, Republic of Korea*
[2]*Department of Electrical Engineering, Korea Advanced Institute of Science and Technology, Daejeon 305-701, Republic of Korea*

(Received 27 April 2015; accepted 28 July 2015; published online 5 August 2015)

We show, using density functional theory (DFT) calculations, that the Schottky barrier height (SBH) at the PtSi/Si interface can be lowered by uniaxial strain applied not only on Si but also on PtSi. The strain was applied to the (001) direction of Si and PtSi, which is normal for the interface. The SBH of the hole is lowered by 0.08 eV under 2% of tensile strain on Si and by 0.09 eV under 4 % of compressive strain on PtSi. Because the SBH at PtSi/Si contact is approximately 0.2 eV, this amount of reduction can significantly lower the resistance of the PtSi/Si contact; thus applying uniaxial strain on both PtSi and Si possibly enhances the performance of Schottky barrier field effect transistors. Theoretical models of SB formation and conventional structure model are evaluated. It is found that Pt penetration into Si stabilizes the interface and lowers the SBH by approximately 0.1 eV from the bulk-terminated interface model, which implies that conventionally used bulk-terminated interface models have significant errors. Among the theoretical models of SB formation, the model of strong Fermi level pining adequately explains the electron transfer phenomena and SBH, but it has limited ability to explain SBH changes induced by changes of interface structure. [http://dx.doi.org/10.1063/1.4928323]

I. INTRODUCTION

Schottky barrier metal-oxide semiconductor field-effect transistors (SB-MOSFETs) are considered one of the important candidates for post-CMOS technology.[1] The heavily doped semiconductor source and drain in the conventional MOSFETs are replaced by metal silicides in SB-MOSFETs. This approach not only reduces the parasitic resistance at contacts with source and drain but also relaxes the constraints imposed by doping-profile control on further scaling down of MOSFETs. However, the performance of SB-MOSFETs is inferior to that of conventional MOSFETs owing to the Schottky barrier (SB) at the source channel and drain channel contacts, which plays a role as the energy barrier for conducting electrons and holes. Extensive efforts have been made to lower the SBH so that the adverse effects of SB that appear as reduced on-state current, decreased sub-threshold swing and poorer switching performance can be avoided. By choosing appropriate metal-silicides, low SBH was achieved (e.g., platinum silicide[2] Φ_p = 0.15-0.27 eV for *p*-MOS and erbium silicide[3] Φ_n = 0.24-0.28 eV for *n*-MOS). However, in order to outperform (show comparable on-state current level with) the conventional MOSFETs, the SBH should be close to 0 eV or even negative.

Over the years, various attempts have been made to lower the SBH at silicon-silicide interfaces to improve the performance of SB-MOSFETs by, for example, dopant segregation,[4] inserting an ultrathin insulator at the interface,[5,6] introducing organic molecules[7] or defects at the interface,[8] and tuning the metal work function using a capping layer or dopant-induced strain.[9–12] The introduction of appropriate dopants at the silicide-silicon interface, e.g., B for PtSi and As for ErSi, known

as dopant segregation,[4] has been successfully implemented. However, dopant segregation needs a high thermal budget and crucially relies on the ability to control the concentration and position of dopants. Additionally, it is difficult to implement in sub-20 nm devices. An inserted ultrathin insulator was able to lower the SBH because it depended on the Fermi level,[5,6] but sufficiently low SBH has never been achieved so far.

We suggest that SBH can be lowered by uniaxial strain applied at both the *channel* and the *source/drain* and that therefore, the strain engineering is applicable for higher-performing SB-MOSFETs. *Ab-initio* calculation results on the variation in the SBH of holes (Φ_p) at PtSi/Si interfaces are provided to support our suggestion. The contact of PtSi and Si (001) was chosen as the test system because of its technological importance in *p*-type SB-MOSFETs, as well as for its better thermal stability and atomically sharp interface.[13] Strain engineering has been used for decades in conventional MOSFET technology to improve the carrier mobility in the conduction channel, so the possibility of SBH lowering was naturally tested in a number of experimental[6] and theoretical[14,15] works that applied strain in the channel region for *n*-type Si or biaxial strain for *p*-type Si. However, to our best knowledge, uniaxial strain in both channel and source/drain has not thoroughly been tested so far. Indeed, the effect of strain on the contact metal has rarely been reported.

We also examined the conventional structural model of the interface and theoretical models of SB formation to construct our computational model and interpret the simulation results. Bulk-terminated contact structures are conventionally used in many computational studies, even though the microscopic structure of the interfaces, such as defects, non-uniformity, and intermixing of metal and semiconductor atoms, affects the SBH.[16–20] We find that the penetration of Pt into the Si side stabilizes the interface more than do bulk-truncated interfaces, and it also lowers the SBH significantly. The SBH values from the theoretical models of SB formation were compared with *ab initio* calculations, and their validity and limitation were discussed. Because theoretical models mostly explain the barrier formation with electronic structure consideration only, the models showed limitations in SBH variation owing to structural changes.

In Section II, we present the computational methodology. In the first part of Section III, we evaluate the validity and limitations of a structural model of a metal-semiconductor interface and theoretical models of SB formation. Variation in SBH by applied strain on Si and PtSi is presented in the second and third parts of Section III, respectively. Finally, we present the main conclusions in Section IV.

II. METHODS

Ab-initio density-functional theory (DFT) calculations were carried out within the generalized gradient approximation (GGA) using the functional proposed by Perdew, Burke and Ernzerhof (PBE).[21] Note that the notorious GGA error in band alignment and band gap will not affect our conclusion because we mainly discuss the variations in SBH by applied strain rather than SBH itself. The Vienna *ab initio* simulation package (VASP) is used for the calculations.[22–24] The electronic wave functions were expanded on a plane wave basis set[25] using a kinetic energy cutoff of 400 eV. Core electrons and nuclei were described by projector augmented wave (PAW) potentials,[26] and 10 and 4 valence electrons on the Pt and Si atoms were used. Reciprocal space sampling was done with $11 \times 11 \times 1$ Monkhorst-Pack[27] k-point mesh for structure optimization. Atomic structure is relaxed until all of the force components on the atoms became smaller than 0.02 eV/Å. Our DFT calculations yield the optimized lattice parameter of 5.47 Å (+0.7 % error) for Si crystals, which agrees well with the experimental value of 5.43 Å, in addition to the a = 5.95, b = 5.67 and c = 3.67 Å (within +2 % error) for PtSi.

We built an interface model structure in which the (001) surfaces of both PtSi and Si were in contact with each other. 1×1 unit cells of Si (5.47 Å × 5.47 Å) were used for the repeated unit in the parallel directions (i.e., (100) and (010) directions) of the interface. Eleven atomic layers of PtSi (approximately 19.65 Å of thickness) and 37 layers of Si (49.22 Å) were alternatively arranged in the periodic supercell (Fig. 1(a)). Two interfaces in the supercell were set to be symmetric in order to minimize the effect of the dipoles that were formed in the asymmetric periodic simulation cell.

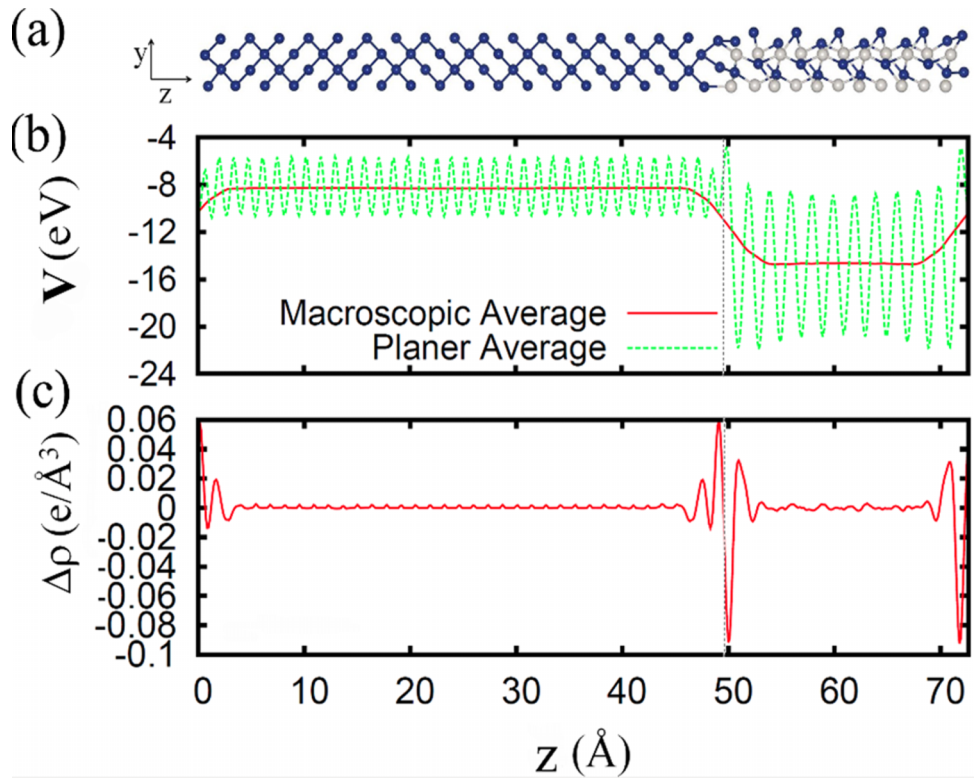

FIG. 1. (a) The relaxed structure of a PtSi/Si supercell, (b) microscopic and macroscopically averaged electrostatic potential energy (in eV) and, (c) changes in electron density from separated PtSi and Si ($\Delta\rho = \rho_{\text{tot}} - \rho_{\text{PtSi}} - \rho_{\text{Si}}$). z is the position along the direction that is normal to the interface. The electrostatic potential energy in the graph is the summation of the ionic potential, which is the local part of pseudopotential (PP) for $r < r_c^{\text{PP}}$, Coulomb potential for $r > r_c^{\text{PP}}$, and Hartree potential.

The Si part was chosen to be thick enough to guarantee the complete decay of the evanescent mode and the metal-induced gap states (MIGS) from the interface so that the electronic density of states (DOS) and electrostatic potential at the central part of the Si channel would become identical to those of Si single crystal (Fig. 1(b)).

Given that the epitaxial growth of PtSi on the Si substrate is assumed in the present work, the lattice constant of PtSi was changed in order to adjust to the Si substrate while the Si lattice constant was unchanged by PtSi. The in-plain supercell size was set to be the same as that of the Si (001), and then the PtSi part was compressed to fit into this supercell. In this structure, PtSi is strained by −3.1 % in the (100) and −8.7 % in the (010) directions, and the resulting strain in the (001) direction (i.e., interface normal direction) is +7 % (c = 3.93 Å). The positions of every atom and the thicknesses of the supercells in the (001) direction were relaxed while 13 layers at the central part of Si were kept fixed. This structure was used as an *unstrained* interface throughout this work because there was no intentionally applied strain. The modeling methods for the strained structure are described in the pertinent sections.

The SBH of holes (Φ_p) is calculated using the following equation rather than reading the difference between the Fermi level (ε_{F}) of the PtSi and the valence band maximum (VBM, E_{V}) from the density of states.

$$\Phi_p = \Delta\bar{V} + \Delta E_{\text{bulk}} = \left(\bar{V}_{\text{PtSi}} - \bar{V}_{\text{Si}}\right)_{\text{slab}} + \left[\left(\varepsilon_{\text{F}} - \bar{V}_{\text{PtSi}}\right) - \left(E_{\text{V}} - \bar{V}_{\text{Si}}\right)\right]_{\text{bulk}} \quad (1)$$

$\Delta\bar{V}$ is the potential lineup term, which is the difference between the macroscopic average of the electrostatic potentials[28] in the bulk type PtSi ($\bar{V}_{\text{PtSi}}$) and Si ($\bar{V}_{\text{Si}}$) regions within the supercell. The band structure term ΔE_{bulk} is the difference between the Fermi level of the bulk PtSi and the valence band maximum of the bulk Si where each is calculated with respect to the averaged electrostatic potential in a corresponding single crystal bulk. In Eq. (1), it is assumed that the Fermi level of

PtSi and the VBM of Si relative to their corresponding electrostatic potential are the same at the single crystal and at the central of each part in slabs (i.e., $\left(\varepsilon_F - \bar{V}_{PtSi}\right)_{bulk} = \left(\varepsilon_F - \bar{V}_{PtSi}\right)_{slab}^{center}$ and $\left(E_V - \bar{V}_{Si}\right)_{bulk} = \left(E_V - \bar{V}_{Si}\right)_{slab}^{center}$). Therefore, the change in SBH is the same as the change in the potential difference $(\bar{V}_{PtSi}\text{-}\bar{V}_{Si})_{slab}$.

Charge neutrality level (CNL) is calculated as below to compare the DFT results with the theoretical models of SB formation. Tersoff's interface dipole theory[29] is used to determine the position of CNL within the silicon band gap. The cell-averaged real-space Green's function is calculated using the following expression[15,29]

$$G(\mathbf{R}, E) = \int_{\Omega} d^3 r g(r, r', E) = \sum\nolimits_{n\mathbf{k}} \frac{e^{i\mathbf{k}\bullet\mathbf{R}}}{E - E_{n\mathbf{k}}}, \tag{2}$$

where $\mathbf{k}$ is the Bloch wave vector, n is the band index, $E_{n\mathbf{k}}$ is the energy of the Bloch state and $\mathbf{R}$ is the lattice vector. The single propagation vector $\mathbf{R}$ ([110] as any disturbance reached farthest along this direction) is chosen, and $\mathbf{k}$ summation is done over the same k-point grid that was used in the self-consistent field calculations of the electronic structures. The contributions of conduction and valence bands to Green's function (in Eq. (2)), i.e., G_C and G_V, are calculated separately, and E_{CNL} is defined as the energy that satisfies the conditions of Eq. (3).

$$G_V(\mathbf{R}, E_{CNL}) = G_C(\mathbf{R}, E_{CNL}) \tag{3}$$

III. RESULTS AND DISCUSSION

A. Evaluation of the structural and theoretical models

The calculated SBH is 0.36 eV of the DFT calculations for unstrained structures, which is larger than experimental observations, 0.15-0.27 eV.[30] We also compared SBH calculated with other exchange-correlation functionals because of GGA error in energy-level alignment. The SBH calculated using local density approximation (LDA)[31] and the Becke-Johnson meta-GGA functional as modified by Tran and Blaha (TB-mBJ)[32] were 0.28 and 0.69 eV, respectively. The PBE result was also corrected using the Heyd-Scuseria-Ernzerhof (HSE06)[33] hybrid functional by modifying Eq (1). as $\Phi_p = \Delta\bar{V}^{PBE} + \Delta E_{bulk}^{HSE}$. The HSE-corrected Φ_p is 0.16 eV. The LDA and HSE results appear to agree with the experimental results. However, lower SBH was found at the more realistic interface structures, as described in the following paragraphs.

We evaluated the bulk-terminated interface model, which is conventionally used in computational studies, using less-abrupt interfaces generated by removing, adding or replacing atoms at the bulk-terminated interface, as shown in Fig. 3. The formation energy of the modified interface by element X (Pt or Si) is defined as

$$\Delta E = (E_{tot} \pm nE_X) - E_0 \tag{4}$$

where E_{tot} and E_0 are the total energies of the modified and bulk-terminated interfaces, respectively, E_X is the per-atom energy of element X in its bulk state, and n is the number of added or removed atoms of X. The negative sign reflects adding X, and the positive sign reflects removing X.

Our results show that many less-abrupt interface structures are more stable than bulk-terminated structures (Table I), and that in particular, the interfaces with monotonically decreasing platinum density at the interface are more stable than other structures. In the 1×1 supercell calculations (Fig. 3(a) and Table I), Pt-I, Pt-sub1 and Pt-sub2 are more stable than bulk-termination. In the doubled-area 2×1 supercell, the structure that platinum density decreases slowly and monotonically (4-3-2-1-0 structure, Fig. 3(b)) is lower in energy than the rapidly or non-monotonically changing structures. Indeed, the SBH of the most stable structures, the Pt-sub1 of the 1×1 supercell and the 4-3-2-1-0 of the 2×1 supercell, are approximately 0.1 eV lower than the bulk-terminated structure. Many experimental studies[34–36] have reported the diffusion of Pt atoms from silicide to silicon, which agrees with our energy formation calculations, which imply that SBH will be lowered by Pt penetration. If the same amount of SBH lowering occurs in other functional calculations, the LDA

and GGA results are in the experimentally measured range, but the TB-mBJ and HSE06 results are out of the range.

We suspect that this inconvenient finding that SBHs from the calculation of less-accurate functionals (LDA and GGA) agree more with experimental observation than do those from the calculation of more-accurate functionals (TB-mBJ and HSE06) comes from the artificial compression of PtSi. PtSi in our periodic supercell calculation is compressed by 5% in volume. As is shown in the section on strain-on-silicide, this amount of compression can lower SBH by roughly 0.1 eV. Therefore, we expect that naturally formed SBH is ~ 0.1 eV higher than our calculations. It is a great coincidence that the SBH lowering by Pt penetration and the error from artificially compressed PtSi nearly cancel each other out in the bulk-terminated interface.

Although we find evidence of error cancellation in the bulk-terminated interface model, there are many questions regarding reliable methods (i.e., structural model and exchange-correlation functional) for SBH prediction. Hence, we restrict ourselves in that not the SBH but the variation in SBH from the unstrained structure is mainly discussed.

We evaluate theoretical models of SB formation by comparing the *ab initio* calculations. Theoretical models of SB formation mostly lie in between the model of strong electronic coupling between metal and semiconductor and the model of no electronic coupling. In SBH without coupling, the Schottky-Mott (SM) model,[37] SBH is the difference between the Fermi levels of PtSi and the ionization energy of Si, which are separately calculated. SBH is calculated to be 0.68 eV, which is much larger than the PBE result in contact geometry (0.36 eV). At the strong coupling limit, known as the Bardeen limit, the Fermi level of metals is pinned at some level in the semiconductor gap, and therefore Φ_p is the difference between VBM and that gap level. Various types of gap states were suggested such as charge neutrality level (CNL),[29] surface states,[38] metal-induced gap states (MIGS),[39,40] defect induced states,[41] and disorder-induced gap states.[42] We consider CNL and MIGS because our structural model has no defects or disorder. Explicit calculation of CNL using equation (3) with Kohn-Sham states shows that the SBH from the CNL model was 0.35 eV. The SBHs for less-strong coupling cases are expressed with parameter S, as shown in the following equation, $\Phi_p = E_G - S(\phi_{PtSi} - E_{CNL}) - (E_{CNL} - \chi_{Si})$, where ϕ_{PtSi} is the work function of PtSi and E_G and χ_{Si} are the band gap and the electron affinity of silicon. $S = 1$ and 0 correspond to the SM model and the CNL model, respectively. The MIGS model for the PtSi/Si interface, using $S = 0.08$ as was obtained in an earlier study,[43] we estimate $\Phi_p = 0.37$ eV. SBH from strong pining models agrees well with the DFT results for the bulk-terminated interface.

Strong pining models capture the electronic effect well but miss the effect from structural changes. MIGS clearly appear at silicon near the interface (Fig. 2). The interface dipole was induced toward PtSi (Fig. 1(c)) because of the electron transfer from PtSi to MIGS of near-interface Si. This dipole will elevate electronic Si energy levels compared with PtSi and lower the Φ_p from the non-pining model. However, the lower SBH by Pt penetration cannot be explained with this model because the SBH in PBE calculations decreases, but it cannot be lowered by changing parameter S in the MIGS model.

B. SBH lowering by strain *on silicon*

After setting our reference at the unstrained silicide/silicon interface in section III A, we now turn to the strained silicon/silicide interface. The effect of strain would be different for the different crystallographic directions of the silicon. In current electronics technology, (100) and (110) channel directions on the (001) surface have been extensively used. In the present work, we strained the Si uniaxially along the (001) direction. Because we were particularly interested in the variation in SBH by applied strain rather than the absolute SBH value, we used bulk-terminated interfaces rather than the modified structures that were discussed in the previous section.

Strain is applied on Si along the (001) direction of conventional cell, and the lattice parameters along two other directions, (100) and (010), are determined using the calculated Poisson ratio. The Poisson ratio is 0.29, which is in good agreement with the experimental value of 0.28 for Si (001).[44] Because epitaxial growth in PtSi is assumed in this study, the PtSi lattice parameter along the interface parallel directions are fixed at a strained Si lattice parameter, and then PtSi is relaxed along

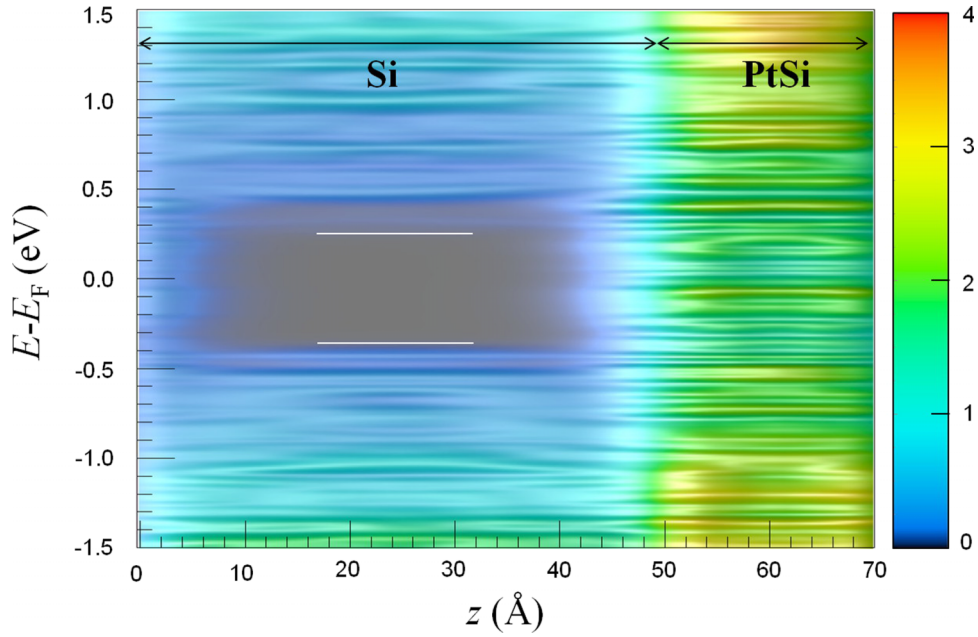

FIG. 2. Density of states with respect to the distance along the z direction. The presence of MIGS is clear. The VBM and CBM of the Si bulk are at -0.36 and 0.25 eV (white lines).

the interface normal direction to release the stress. Thirteen layers of the Si central part were fixed, but supercell thickness and other atoms close to the interface were relaxed.

SBH is lowered by uniaxial strain regardless of strain direction, as Fig. 4 shows. Φ_p lowering can be explained either by narrowing the band gap (E_G^s) of Si in the CNL model or by decreasing the ionization energy (IE) in the SM model (Table II). Strain breaks the tetragonal symmetry of Si bonds, and the degeneracy of bands is lifted. Table II shows that E_G^s and IE decrease when strain is applied. Variations in E_G^s and IE, as with variations in the CNL, change the barrier height. In the CNL model, the uniaxial strain decreases the SBH (E_V-E_{CNL}) up to 0.14 eV for 2% compressive strain. Earlier theoretical studies also found similar decreases in SBH irrespective of the direction of applied strain,[14] although quantitative matching was not possible because these studies looked at bi-axial strain. The trends in SBH changes from PBE calculations and model calculations are in-line with each other, but both the CNL and the SM models exaggerate SBH change.

TABLE I. Formation energies (ΔE) of various modified interfaces (with element X) are given in eV. Modified sites are displayed in Fig. 3. Pt-sub2 is the structure made by substituting the Si2 site. In the 2×1 supercell, only interstitial Pt atoms were considered owing to computational demands. The integers in the structure name of the 2×1 supercell are the number of Pt atoms at each atomic layer per 2×1 unit cell (4 for PtSi and 0 for Si).

1×1 supercell			2×1 supercell	
type	Site	ΔE	structure	ΔE
V	Pt1	2.46	4-1-0	0.12
V	Pt2	1.35	4-2-1-0	-0.76
V	Si1	1.13	4-3-1-0	-1.88
V	Si2	0.85	4-3-2-1-0	-3.18
I	Pt-I	-0.64	4-2-3-1-0	-2.54
S	Pt-sub1	-0.89	4-0-2-0	0.28
S	Pt-sub2	-0.80		

V= vacancy, I= interstitial, S= substitution

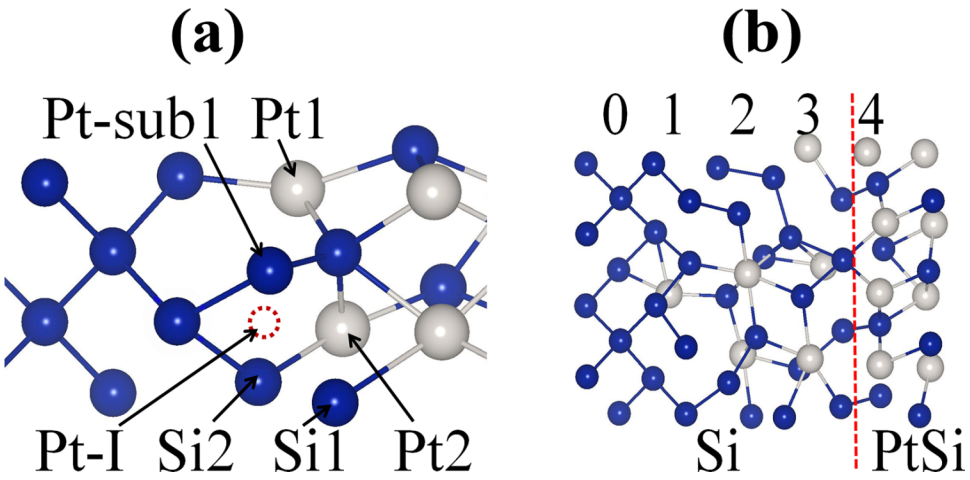

FIG. 3. (a) Labels are used for various modified interfaces (in the 1×1 supercell) that were considered in Table I and (b) for the lowest energy structure of 2×1 supercell calculations, denoted as a 4-3-2-1-0 structure with linearly decreasing density of Pt atoms. Pt1, Pt2, Si1 and Si2 indicate the vacancy cites for the modified interfaces. Pt-I (red dotted circle) is the interstitial Pt atom at a distance of roughly 2.5 Å from the Pt2. Pt-sub1 and Pt-sub2 (in Table I) represent Pt atoms that substitute Si atoms marked as Pt-sub1 and Si2, respectively. Blue and gray balls represent Si and Pt atoms, respectively.

We analyze the effects of electronic and structural relaxation at the interface on SBH variation one by one. We began with the Schottky-Mott model, which ignores electronic relaxation as well as structural relaxation at the interface. The work function of PtSi and ionization energy of Si were calculated separately under applied strain in this step (Table II). Earlier studies demonstrated that metal's work function increases with compressive biaxial strain and decreases with tensile strain,[8] which agrees with our calculations. As shown in Table II, the IE of silicon decreases and E_V moves

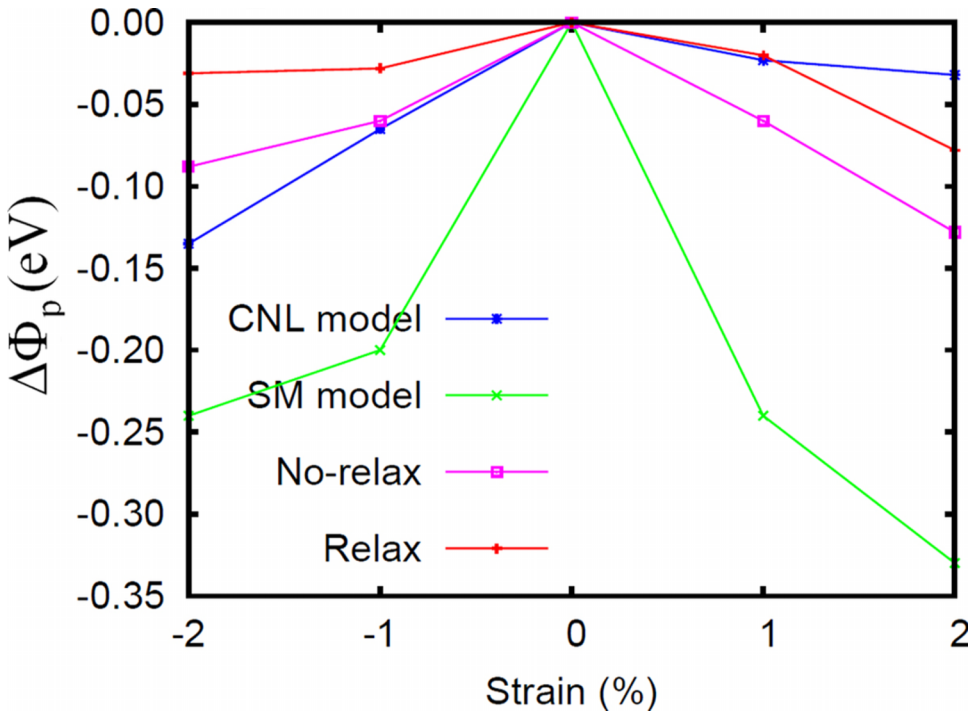

FIG. 4. The variation in SBH ($\Delta\Phi_p = \Phi_p^S - \Phi_p^0$) with applied strain on Si. Φ_p^S and Φ_p^0 are the SBH values of strained and unstrained structures. The "SM model" was reserved for no electronic or structural relaxation, "No-relax" is for without structural relaxation, and "Relax" is for relaxed atomic structure calculation.

TABLE II. Band gap of strained bulk Si (E_G^s), work function of PtSi (ϕ) and ionization energy (IE) of Si of the strained Si. ϕ and IE are evaluated using 11-layer PtSi and 25-layer Si slabs, respectively. The band gaps at both PBE and TB-mBJ (in parenthesis) level are given.

Strain (%)	E_G^s (eV)	ϕ (PtSi)	IE(Si)
-2	0.33 (0.87)	4.78	5.22
-1	0.47 (1.02)	4.80	5.27
0	0.62 (1.17)	4.80	5.48
1	0.56 (1.11)	4.83	5.27
2	0.50 (1.05)	4.86	5.21

Units are in eV.

upward irrespective of the direction of applied strain, and the IE reduces SBH, but by too much (Figure 4).

In the second step, we relax the electronic density at the interface. SBH was calculated using contact geometry of PtSi and Si slabs separated by the minimum energy distance between rigid Si and PtSi ('No-relax' in Fig. 4). In this step, the positions of atoms were not relaxed but were fixed at their respective positions in the bulk. Electronic relaxation weakens changes in SBH. Large difference in the electronic chemical potential of PtSi and Si induces electron transfer from PtSi to Si, and the resultant interface dipole partially compensates for the change of Φ_p. The mechanism of SB formation in this step is conceptually comparable with that from the CNL model; however, there is a mismatch between the CNL model and the *ab initio* calculations.

In the last step, we consider the effect of atomic structure relaxation at the interface. As is shown in Fig. 4, structural relaxation further weakens the SBH lowering from the level by which it was lowered through electronic relaxation. Interestingly, SBH for tensile strain agrees well with CNL models, but they differ greatly regarding compressive strain; Φ_p for −2, 0, and 2 % strains are 0.33, 0.36 and 0.28 eV in the PBE calculations and 0.22, 0.35, and 0.32 eV in the CNL model. These findings may refer to the effects of asymmetric structural change in compressive and tensile strain. Tensile strain, rather than compressive strain, seems to have more effect on SBH lowering; Φ_p is lowered by as much as 0.07 eV for 2 % tensile strain, but it is lowered by 0.03 eV for 2 % compressive strain. The findings also imply that the strain on silicon improves the performance of SB-MOSFET not only by improving hole mobility (because of reduced inter-valley scattering) in the channel but also because of lowering the SBH.

C. Change of SBH by strain-*on-silicide*

As a different option from the conventional approach of strain-on-silicon, we also attempted to use strain-on-silicide to determine whether strain engineering was applicable to electrodes. Uniaxial strain was applied on PtSi along the (001) direction, normal to the interface. Because of our assumption about the epitaxial growth of the PtSi thin layer on the Si substrate, the lattice dimensions of PtSi along the direction parallel to the interface are fixed at unstrained Si lattice parameters; only the cell size of PtSi in the normal interface direction is changed according to the applied strain. All Si atoms were fixed except two layers at the interface.

SBH changes almost linearly with respect to the applied strain on PtSi (Fig. 5). It increases by approximately 50 meV with 4% of tensile strain and decreases by 90 meV with the same magnitude of compressive strain. Because the SBH of PtSi/Si is 0.15-0.27 eV,[2] 0.09 eV lowering may lower SBH to less than 0.1 eV, which is the condition for SB-MOSFETs to outperform conventional MOSFET. Indeed, the monotonic behavior of SBH will lead to easier tuning.

It is surprising that SBH is decreased under compressive strain. The SBH of holes can be expressed as[45] $\Phi_p = (\mathrm{IE} - \phi) - 4\pi D_{\mathrm{int}}$, where D_{int} is the electric dipole density at the interface. The Fermi level of a metal usually elevates under compressive strain because electron density increases. The elevation of the Fermi level increases IE − ϕ. At the same time, it enhances the interface dipole term by inducing the transfer of more electrons from PtSi to Si, and, as a result, the change in

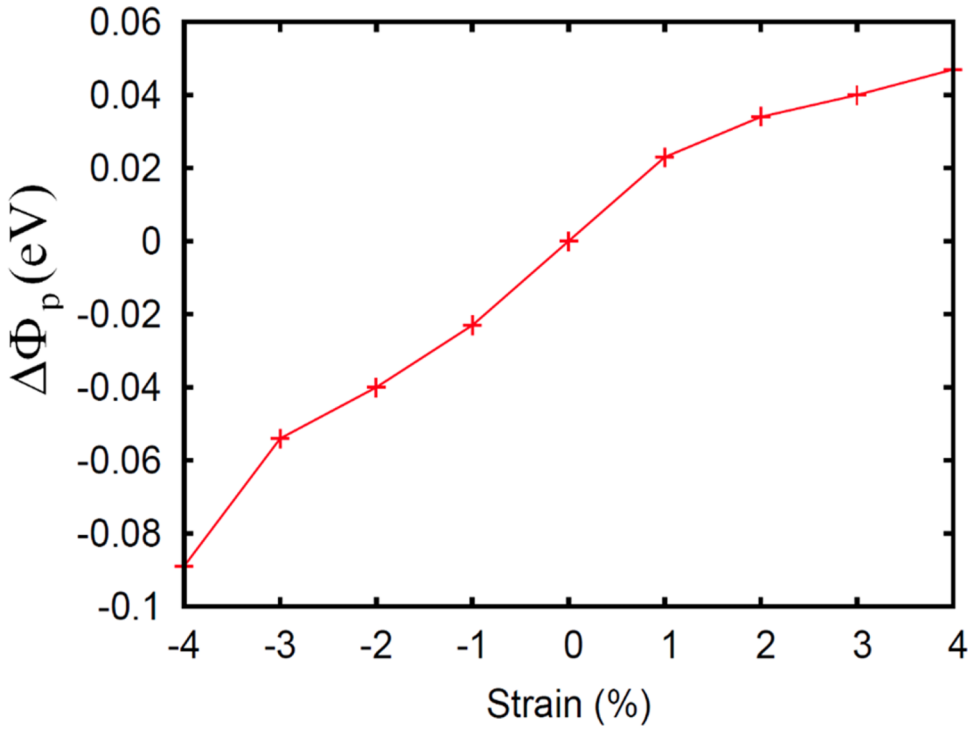

FIG. 5. The variation in SBH ($\Delta\Phi_P = \Phi_P^S - \Phi_P^0$) by applied strain on PtSi. Positive and negative values represent tensile and compressive strain, respectively.

SBH decreases. It is natural to expect that SBH changes by interface dipole would be smaller than the Fermi level changes because the Fermi level change is the cause of enhancing the dipole, and therefore Φ_p was expected to increase under compressive strain. The opposite is expected for tensile strain. This unexpected observation may imply the importance of non-electronic effects such as structural changes.

Our calculations imply that strain-on-silicide can also be employed to tune the SBH at the PtSi/Si interface. SBH's flexibility in being able to can be lowered depending on the direction of applied strain can help in achieving low SBHs for both electrons and holes using the same metal. Although our model structure is quite far from the real interface in SB-MOSFETs, we believe that our results of SBH tuning using *strain-on-silicides* will motivate engineers to verify and, if they are successful, to implement SB-MOSFETs.

IV. CONCLUSIONS

In conclusion, we report the effect of strain applied on silicon or silicide on SBH at a PtSi/Si (001) interface. Irrespective of the direction of applied strain on Si, SBH decreases with the increasing strength of strain when strain is applied on the Si channel, whereas SBH changes almost linearly with the strain applied on PtSi. The predicted decreases in SBH are 0.07 eV for 2% tensile strain on Si and 0.09 eV for 4 % compressive strain on PtSi. It is found that structural and electronic relaxations at the interface weaken the SBH change. We also demonstrate the importance of interfacial structure in the barrier formation. In particular, we find that Pt penetration into the Si stabilizes the interface and lowers the SBH by at least 0.1 eV compared with bulk-terminated interfaces, which implies that theoretical studies that use conventionally used bulk-terminated interfaces have significant errors even when they apparently agree well with experimental observations. Given that we have shown that strain on both Si and PtSi can lower the SBH, it might be possible to develop higher-performing SB-MOSFETs by strain control. Especially, strain on silicide can

provide another way to improve the performance given that strain on sources and drains is not conventionally used in current semiconductor technology.

ACKNOWLEDGEMENTS

We acknowledge that P.S., H.M., K.-R.L., and S.K. were supported by the Korea Institute of Science and Technology (KIST) through the Institutional Project (Grant No. 2E25372), and M.S was supported by the Pioneer Research Center Program through the National Research Foundation of Korea (NRF) funded by the Ministry of Science, ICT Future Planning (NRF-2011-0027906). Computational resources were provided by the Institute of Materials Research (IMR) at Tohoku University, Japan.

[1] J. M. Larson and J. P. Snyder, IEEE Trans. Electron Devices **53**, 1048 (2006).
[2] J. B. Bindell, W. M. Moller, and E. F. Labuda, IEEE Trans. Electron Devices **27**, 420 (1980).
[3] M. H. Unewisse and J. W. V. Storey, J. Appl. Phys. **73**, 3873 (1993).
[4] M. Zhang, J. Knoch, Q. T. Zhao, U. Breuer, and S. Mantl, Solid-State Electronics **50**, 594 (2006).
[5] D. Connelly, C. Faulkner, D. E. Grupp, and J. S. Harris, IEEE Trans. Nanotechnol **3**, 98 (2004).
[6] M. H. Liao, P.-S. Kuo, S. R. Jan, S. T. Chang, and C. W. Liu, Appl. Phys. Lett. **88**, 143509 (2006).
[7] J. R. Heath and M. A. Ratner, Phys. Today **56**, 43 (2003).
[8] T. Tamura, S. Ishibashi, K. Terakura, and H. Weng, Phys. Rev. B **80**, 195302 (2009).
[9] S. Guha and V. Narayanan, Annu. Rev. Mater. Res. **39**, 181 (2009).
[10] J. A. Rothschild, A. Cohen, A. Brusilovsky, L. Kornblum, Y. Kauffmann, Y. Amouyal, and M. Eizenberg, J. Appl. Phys. **112**, 013717 (2012).
[11] M. K. Niranjan and U. V. Waghmare, J. Appl. Phys. **112**, 093702 (2012).
[12] S. Toyoda, H. Kumigashira, M. Oshima, H. Sugaya, and H. Morita, Appl. Phys. Lett. **100**, 112906 (2012).
[13] R. T. Tung, J. M. Gibson, and J. M. Poate, Phys. Rev. Lett. **50**, 429 (1983); Appl. Phys. Lett. **42**, 888 (1983).
[14] C. Ohler, C. Daniels, A. Förster, and H. Lüth, Phy. Rev. B **58**, 7864 (1998).
[15] A. Yagishita, T.-J. King, and J. Bokor, Jap. J. App. Phy. **43**, 1713 (2004).
[16] N. V. Rees and C. C. Matthai, Semicond. Sci. Technol. **4**, 412 (1989).
[17] N. V. Rees and C. C. Matthai, J. Phys. C: Solid State Phys. **21**, L981 (1988).
[18] J. Bardi, N. Binggeli, and A. Baldereschi, Phy. Rev. B **59**, 8054 (1999).
[19] C. Berthod, N. Binggeli, and A. Baldereschi, Phy. Rev. B **68**, 085323 (2003).
[20] C. Berthod, N. Binggeli, and A. Baldereschi, Europhys. Lett. **36**, 67 (1996).
[21] J. P. Perdew, K. Burke, and M. Ernzerhof, Phys. Rev. Lett. **77**, 3865 (1996).
[22] G. Kresse and J. Hafner, Phys. Rev. B: Condens. Matter **47**, RC558 (1993).
[23] G. Kresse and J. Furthmüller, Comput. Mater. Sci. **6**, 15 (1996).
[24] G. Kresse and J. Furthmüller, Phys. Rev. B: Condens. Matter **54**, 11169 (1995).
[25] J. Ihm, A. Zunger, and M. L. Cohen, J. Phys. C: Solid State Phys. **12**, 4409 (1979).
[26] P. E. Blöchl, Phys. Rev. B **50**, 17953 (1994).
[27] H. J. Monkhorst and J. D. Pack, Phys. Rev. B. **13**, 5188 (1976).
[28] N. Binggeli and A. Baldereschi, J. Phys. D **31**, 1273 (1998).
[29] J. Tersoff, Phys. Rev. Lett. **52**, 465 (1984).
[30] E. Dubois and G. Larrieu, J. Appl. Phys. **96**, 729 (2004).
[31] J.P. Perdew and A. Zunger, Phys. Rev. B **23**, 5048 (1981).
[32] F. Tran and P. Blaha, Phys. Rev.Lett. **102**, 226401 (2009).
[33] J. Heyd, G. E. Scuseria, and M. Ernzerhof, "Hybrid functionals based on a screened coulomb potential," J. Chem. Phys. **118**, 8207 (2003).
[34] H. Carchano and C. Jund, Solid-state Elec. **13**, 83 (1970).
[35] S. Mantovani, F. Nava, C. Nobili, and G. Ottaviani, Phy. Rev. B **33**, 5536 (1986).
[36] P. Hazdra and J. Vobecký, Mat. Science and Eng. B **124**, 275 (2005).
[37] W. Schottky, Z. Phys. **113**, 367 (1939).
[38] J. Bardeen, Phys. Rev. **71**, 717 (1947).
[39] V. Heine, Phys. Rev. **138**, A1689 (1965).
[40] C. Tejedor, F. Flores, and E. Louis, J. Phys. C **10**, 2163 (1977).
[41] W. E. Spicer, P. W. Chye, P. R. Skeath, C. Y. Su, and I. Lindau, J.Vac. Sci. Technol. **16**, 1422 (1979).
[42] H. Hasegawa and H. Ohno, J.Vac. Sci. Technol. B **4**, 1130 (1986).
[43] M. K. Niranjan, S. Zollner, L. Kleinman, and A. Demkov, Phy. Rev. B **73**, 195332 (2006).
[44] M. Mongillo, P. Spathis, G. Katsaros, and S. De Franceschi, Phy. Rev. X **3**, 041025 (2013).
[45] R. T. Tung, Appl. Phys. Rev. **1**, 011304 (2014).